Smart Materials, Magnetic Graphene Oxide-Based Nanocomposites for Sustainable Water Purification

Janardhan Reddy Koduru, Rama Rao Karri and N. M. Mubarak

1 Introduction

Water pollution is a global environmental concern [61–64, 75]. Heavy metals are one of the primary contaminants in the aqueous environment. Continuous exposure to heavy metals leads to high-risk health problems for humans. Heavy metals are naturally occurring throughout the Earth's crust [2]. Anthropogenic activities, including mining operations, industry, and the use of metals and metal-containing compounds for the domestic and agricultural purpose, are the main sources of water pollution [83]. Hence, water is one of the major routes through which heavy metals and radionuclides may enter the human body [22]. Figure 1 shows the possible sources of water pollution. The real application of frequently used conventional wastewater purification techniques is limited to the removal of heavy metals at trace levels [22]. However, the low installation cost and easy operation of adsorption technique make it one of the preferred methods for water purification [26, 40, 25, 27]. Moreover, the use of activated carbon in the adsorption process is effective, but the use of it in a real application is limited, due to the complex installation process, coupled with the high-cost operation [41]. Hence, these drawbacks have

J. R. Koduru
Department of Environmental Engineering, Kwangwoon University, Seoul 01897, Republic of Korea
e-mail: reddyjchem@gmail.com

R. R. Karri (✉)
Petroleum and Chemical Engineering, Faculty of Engineering, Universiti Teknologi Brunei, Gadong, Brunei Darussalam
e-mail: kramarao.iitd@gmail.com

N. M. Mubarak
Department of Chemical Engineering, Faculty of Engineering and Science, Curtin University, 98009 Miri, Sarawak, Malaysia
e-mail: mubarak.mujawar@curtin.edu.my

Inamuddin et al. (eds.), *Sustainable Polymer Composites and Nanocomposites*,
https://doi.org/10.1007/978-3-030-05399-4_26

necessitated the search for an alternative material that can be renewable and economic for water purification. The various potential applications of GO-based nanocomposites have been reported by different research groups [37]. Both the chemical stability of magnetic GO-based nanocomposites and literature survey, induce us to write a book chapter on magnetic GO (MGO's) based nanocomposites for the removal of heavy metals and radionuclides from water, with the purpose of reducing their environmental impact.

The numerous merits of graphene, which include high specific surface area, and thermal conductivity, high optical transmittance, and large Young's modulus have led to researchers paying great attention to it [78]. Similar to graphene, graphene-based material or graphene oxide (GO) shows the above significant properties. "However, GO is more easily dispersed than graphene, due to the presence epoxy, hydroxyl, and carboxyl functional groups, thus making its processing, synthesis, and application more convenient" (Fig. 2) [11]. Due to its imperishable hydrophilicity, GO found to be an efficient adsorbent and hence found many applications, including water purification [11]. Sreeprasad et al. [77] and Maaz et al. [47] have reported that nickel ferrite-GO composite is a better reaction media than iron ferrites, because of having higher catalytic and electron transfer efficiency through the Ni^{2+} in the nickel ferrite. Moreover, previous reports have proved the amazing removal response of magnetic nanoparticles/graphene or GO composites for pollutants like chromium [17, 67], copper [20], arsenic [105], cadmium [14], lead [100], and cobalt and an organic dye. Recently, Ligamdinne

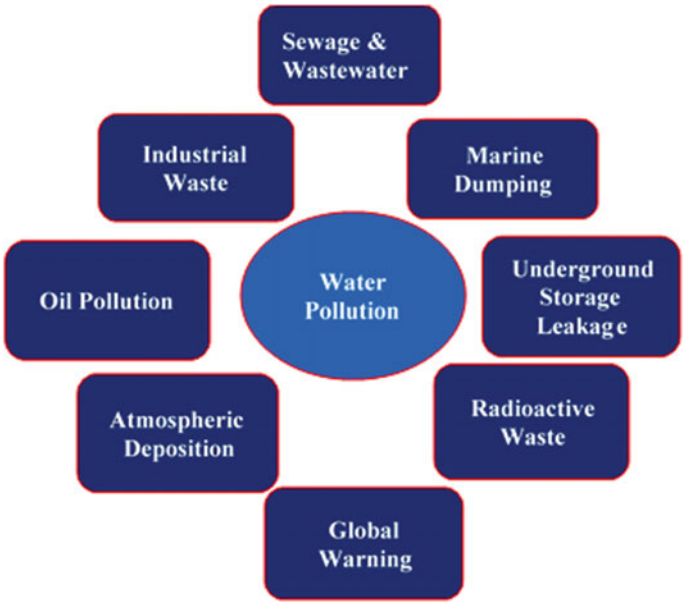

Fig. 1 Schematic of the sources of water pollution

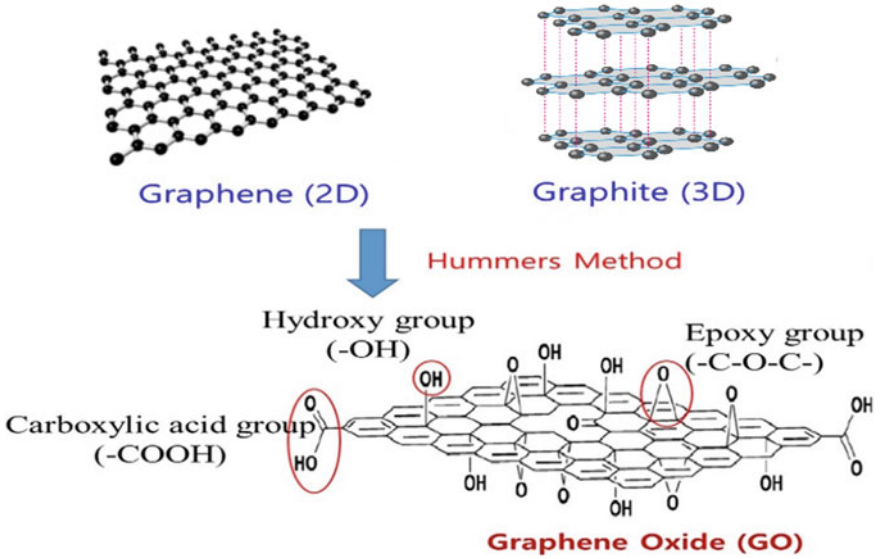

Fig. 2 Graphical representation of graphene oxide (GO) produced from graphite

et al. reported (Fig. 3) the removal of Co(II), Pb(II), Cr(III), As(III) and As(V), and radionuclides, U(VI) and Th(IV) from water, using the synthesis of "inverse spinel nickel ferrite incorporated-graphene oxide" based nanocomposites [35, 36, 39, 40]. The reported results demonstrated that the magnetic GO-based nanocomposites are promising, economic, could be separated by the external magnetic field.

Graphene can be extracted from graphite and it is merely a sheet of graphite [65]. It is defined as a single layer of sp^2 bonded carbon atoms in hexagonal lattice arrangement [97]. At the same time, graphene possesses few promising properties such as good electronic properties caused by the bonding and anti-bonding of the pi orbitals. Furthermore, graphene is clarified to be the strongest substance in terms of mechanical strength since it possesses high tensile strength and it is light in weight. For instance, it is more than 40 times stronger than diamond and more than 300 times stronger than A36 structural steel, at 130 GPa [81]. Meanwhile, for the optical properties, high absorption of white light up to 2.3% is capable to be observed from graphene.

Besides the impressive properties, appropriate method to produce graphene must be taken into consideration. There are two different type of methods to produce graphene which are exfoliation methods and direct growth of graphene layer [30]. Methods to generate graphene include "Scotch Tape Method", dispersion of graphite, exfoliation of graphite oxide, epitaxial growth and lastly CVD [23]. However, improved Hummers method which falls under the method of dispersion of graphite is used since it is an improved method which reduces the toxic gas emission and at the same time enhances the reaction performance [50].

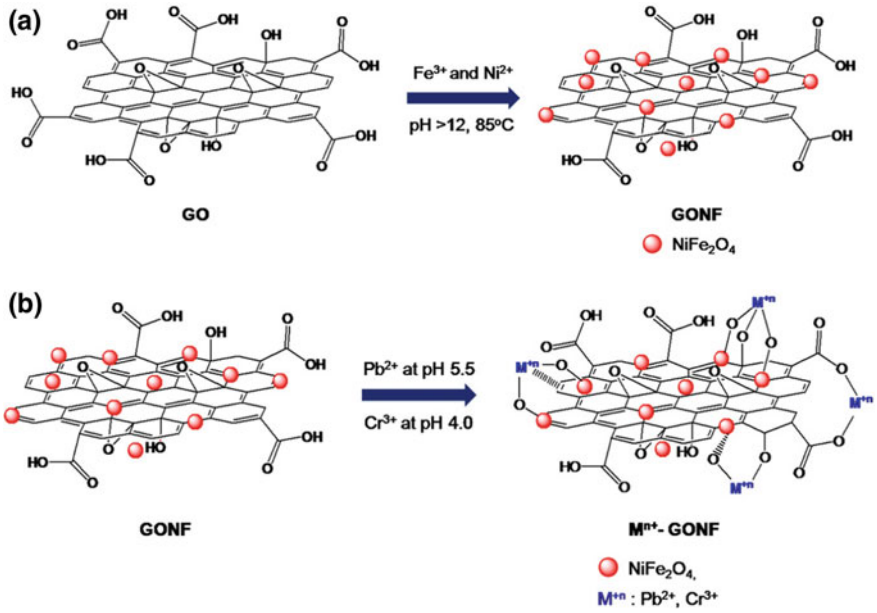

Fig. 3 Graphical representation of **a** nano-magnetic GONF composite preparation, **b** Pb(II) and Cr(III) adsorption onto GONF (reproduced from [39] with permission)

Generally, graphene generated via improved Hummers method are prepared to be further functionalized as chemical functionalization of graphene can be one of the best approaches for cadmium removal [101]. However, before functionalization takes place, the GO can be further transformed into GNs via acid treatment. Functionalization can be defined as the route where the addition of new properties, purposes, structures, or abilities to a substance via the alteration of the material in the aspect of surface chemistry. It is acknowledged that this is an essential method utilized throughout different fields such as biological engineering, chemistry, nanotechnology, materials science and the likes [93]. Functionalization can be done through the attachment of particles or nanoparticles to the surface of a substance, either via a chemical bond or via adsorption. For instance, the functionalized graphene can be produced via noncovalent and covalent alteration techniques. Both techniques share a similar process which is a superficial alteration of GO followed by reduction.

However, functionalization via ionic liquids (ILs) [48, 59] is known as a better covalent bonding technique [69]. The term of IL can be explained as poor coordination of the ions can be found in the salt below 100 °C or at room temperature. Ions in IL avoid the creation of a stable crystal lattice by having at least an ion which the charge is undergone delocalization and an organic component. Properties which include solubility of starting materials and other solvents, melting point, and viscosity are dependent on the counter ion and organic component [66]. For

instance, implementation of ILs for synthetic difficulties is common and hence ILs can be known as "designer solvents". Furthermore, one of the promising advantages of IL is the zero presence of volatility. This condition has resulted in the solvents to have less toxicity compared to low-boiling-point solvents. For instance, by covalent bonding approach, GO obtained via modified Hummers method can be further functionalized via IL such as BF_4 [Bmim] with magnetic Fe_3O_4 nanoparticles to form core-shell structured Fe_3O_4@GO nanospheres to perform optimal extraction of cadmium [1].

2 Properties of Graphene

2.1 Electrical and Electronic Properties

The revolution of graphene can be initiated with the electronic and electrical properties of graphene [51]. Electrical conductivities of graphene, modified graphene and modified graphene/iron pentacarbonyl porous films with composites of chitosan (5, 10, 15, and 30 wt%) are shown in Fig. 4a. It is noted from these graphene derivatives that as the chitosan composite wt% is increased, it lowered the electrical conductivity. The number of layers existing in the graphene is the major factor to affect the properties. Hence, different materials are illustrated for monolayer, bilayer, and tri-layer of graphene. Former studies on graphene have proven that probability of altering charge carriers from holes to electron has led to the possible application in transistors [52]. However, merely monolayer graphene is valid for the electron-hole dependence. Yet, the dependence will get poorer with the disturbance of electrical field transmission by other layers once the number of layers is experiencing increment. The tremendously high mobility of electron at

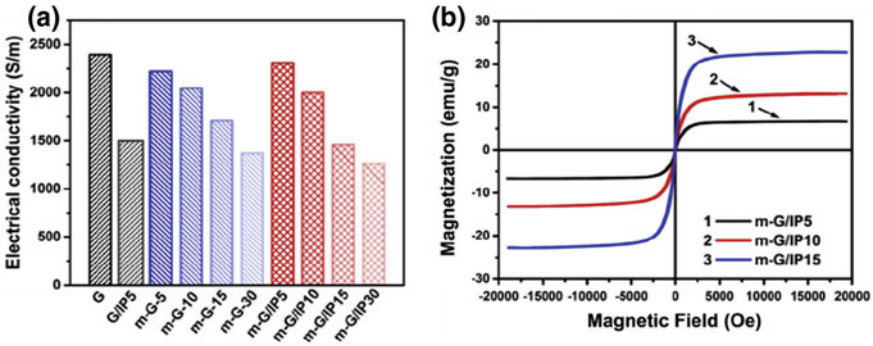

Fig. 4 **a** Electrical conductivities of graphene and its derivative films; **b** hysteresis loops of m-G/IP porous films [G—graphene; m-G—modified graphene, and m-G/IP modified graphene/iron pentacarbonyl porous films; m-GO-X, m-GO/IPX are composites of chitosan (5, 10, 15, and 30 wt%) with m-G and m-G/IP] (reproduced from [42] with permission from Elsevier)

different temperatures and exposure to magnetic fields result in the existence of quantum Hall effect in graphene for the hole and electron carriers [102]. For instance, mechanically generated graphene is found to exceed 2000 cm^2/V s at room temperature. Furthermore, in graphene, it only happens at only half integers of quantum Hall effect instead of happening in the classic integer which is at 4 e^2/h where the electron charge represents e while Planck's constant represents h. This circumstance results from the special band structure of graphene. Besides, utilized substrate and temperature are the major components to affect the performance of electron mobility within graphene. For instance, staggering mobility of suspended and annealed graphene onto Si/SiO_2 can reach more than 200,000 cm^2/V s which is considered as the highest recorded value among all the semiconductor substances [7].

2.2 Magnetic Properties

Magnetic properties of graphene might be affected by the presence of different types of defects [68]. The defects consist of topological defects, point defects, and extended defects. For instance, topological defects can be caused from the shapes such as heptagons and pentagons while the point defects are like adatoms, vacancies and the likes. However, extended defects include edges, voids, and cracks. Besides, defective parts like wrinkles, corrugations, and ripples can be found on the graphene surface. The defective lattice of the graphene such as voids and cracks will result in developing the local magnetic moments and forming interactions between the moments such as ferromagnetic [87]. The connection between the magnetic moments is ferromagnetic or antiferromagnetic if there is a detection of one Bohr magneton of magnetic moment formed by the vacancy or hydrogen chemisorption defects [95]. However, for the disorderly arranged graphene, induction of ferromagnetism can merely be done by monoatomic defects [94]. Furthermore, magnetism can be generated from adatoms, vacancies, and substitutional atoms [85]. In addition, induction of magnetic moment can be done by adding the monovalent and divalent adatom on graphene. The hysteresis loops of m-G/IP porous films with different chitosan composites (5, 10, and 15 wt%) is shown in Fig. 4b. Few studies also demonstrate that magnetism in graphene can be generated by zigzag edges and von Hove singularities [29]. Numerous experiments and methods have been tested regarding the magnetic properties and one of the studies states that reduced graphene oxide by using hydrazine continued by thermal treatment can form ferromagnetism in graphene [89]. Furthermore, exfoliation of graphite via ultrasonic technology in organic solvents can generate the magnetic properties in graphene nanocrystals with a minimum number of defects but no detection of ferromagnetism is observed at the temperature below than 2 K [72]. On the other hand, the presence of ferromagnetism can result from the high concentration of defects and it can be found mostly in the partly hydrogenated epitaxial graphene [91].

2.3 Chemical Properties

Pristine graphene sheets are regularly not reactive. Hence, graphene sheets should undergo superficial functionalization to activate its reactivity. This condition has illustrated that the domination of the surface is significant on the graphene chemistry while the graphene nanoribbons are dominated by the edges. Graphene reactivity also depends much on the thickness. As an example, monolayer graphene is found to have higher reactivity such as 10 times more than that of bilayer or multilayer graphene [73]. This statement is proved by utilizing the Raman spectroscopy in the peak measurement of relative disorder. Comparison of bulk graphene with graphene edges in terms of reactivity via spectroscopy examination is taken place and the discovery is that at least two times higher reactivity is found in the edges than that one of bulk monolayer graphene sheet [57].

2.4 Mechanical Properties

Performance and stability of the practical applications will be inevitably affected by the externally applied stress and unnecessary strain. The crystal-like graphene which covers an interatomic distance will eventually be affected by the externally applied stresses and hence it leads to the redistributed local charge. Indirectly, electronic transport will be varied significantly because of the developing band gap discovered in electronic structure. Anticipations from researchers can be witnessed once graphene is proven to have better performance than CNT in terms of its high stiffness and strength [12]. Hence, atomic force microscope has been utilized to make elastic properties measurement of the single layer graphene. As a result, 1 ± 0.1 TPa of Young's modulus and 130 ± 10 GPa of inherent strength are obtained [5]. Besides, measurement of strain with the applied tension and compression loads to the single layer graphene via Raman spectroscopy is recorded at the value of 1.3% for the strain and 0.7% for the compression and tension correspondingly [84]. There is a different degree of Young's modulus and fracture strength for a different layer of graphene. For instance, 1.02, 1.04 and 0.98 TPa of Young's modulus and 130, 126 and 101 GPa of fracture strength are owned by the single layer, bilayer, and tri-layer graphene correspondingly [31]. Therefore, it is obvious that increment of the layers will directly cause the increment in sliding tendency but weaken the properties. Furthermore, measurement of the alteration in 2D peaks and G with the presence of external stress can be made via Raman spectroscopy to record the measurement of the strains within the graphene sheets due to compression and tension. Potential to alter the band gap has been discovered by the introduction of measured strains because electric band structure can be varied by strain. Implementation of hydrogen plasma to carry out the reduction of graphene oxide has successfully led to the production of modified graphene with Young's modulus of 0.25 TPa [18]. Besides, the fracture toughness of pure

graphene is recorded at 4 MPa since the potential formation of agglomerates and brittle nature due to imperfect graphene are present [99]. In short, reduction of the properties is highly depending on the increment of graphene nanosheet layers.

2.5 Thermal Properties

Phonon transport is the significant variable to affect the performance of graphene in terms of thermal conductivity [106]. Phonon transport can be explained as the ballistic and diffusive conduction at low and high temperature correspondingly. Yet, transport of electronic thermal can be ignorable since the non-doped graphene possesses carrier density which is low. The inherent thermal conduction of graphene can reach to approximately the range from 2000 to 6000 W/mK for the graphene sheets to undergo suspension at room temperature [3]. However, the value of 600 W/mK is recorded for the graphene which is undergoing suspension via silicon dioxide substrate [71]. On the other hand, localization and phonon scattering can take place due to the graphene defects which include isotopic doping [24], edge scattering and sample production deposits [56]. Thus, the guaranteed high quality of graphene sheets generated via micromechanical cleavage approach results in better thermal conduction. Besides, the thermal conductivity of the mechanically exfoliated graphene was recorded within the range of 4800–5300 W/mK [4]. The thermal conductivity is clearly outstanding than that of multi-wall, natural diamond and single wall CNTs which are 3000, 2200 and 3500 W/mK respectively [57]. This has proven that the outstanding thermal conductivity of graphene is most likely to replace the usage of copper.

3 Preparation Methods of MGO Nanocomposites

Most of the MGO nanocomposites are synthesized using the hydrothermal method. Although the hydrothermal process is generally carried out at high temperatures, this technique is an eco-friendly and economically feasible method [19]. Based on the synthetic approaches of MGOs, this hydrothermal method is performed in the presence of organic molecules as precursors and in the presence of alkaline media. The hydrothermal method used to perform at a temperature between 160 and 180 °C in a Teflon-line autoclave [80], is also known as the solvothermal method. Cheng et al. [10] reported: “one-step fabrication of magnetic GO composite gel” for the efficient adsorption removal of dye. The preparation of GO magnetic gel involved the hydrothermal method in the presence of alkaline (NH_3–H_2O) and polymer (polyvinyl alcohol). The gel exhibited both enhanced adsorption removal capacity towards cationic and anionic dyes, and magnetic separation capability, compared with the bare GO [86]. Generally, the ultra-sonochemical method is used to prevent re-aggregation, and improve the dispersion and reduction of the size of

the material. It was used mostly before or after the synthesis of MGOs by the hydrothermal method. The main principle of the solvochemical method is the generation of ultrasound using a titanium horn that can serve to reduce the Van der Waals forces in the GO by ultra-sound irradiation of liquid [55]. Szabo et al. successfully prepared MGOs by sonication of a mixture of magnetic nanoparticles and GO solution [82].

Lately, microwave synthesis has become of great significance in the preparation of inorganic nanomaterials. In the synthesis of inorganic nanomaterials, compared to conventional heating technique, the microwave synthesis technique consumes less energy, environmentally friendly, and provides a homogeneous heating process for speedy reaction [74]. It can also offer rapid and selective heating of the reactant to a high temperature that leads to the production of "self-generated pressure in the sealed reaction vessel" [82]. Some of the previous works used the microwave synthesis method for the preparation of MGOs, including Mn_3O_4-rGO nanocomposites [74], and GO-NiO·4ZnO·4CoO·2Fe_2O_4 nanocomposites [45].

4 Structural Characterization and Properties of MGOs

The formation and structural functionalities of the prepared GO's and MGOs can be characterized using spectroscopic techniques that include XRD, XPS and FT-IR, and RS. The surface morphology, size, porosity, and dimensions of the prepared GO's and MGOs were evaluated using microscopic techniques, including AFM, TEM, and SEM. The surface area and surface primary adsorption characteristics were evaluated using BET theory analysis. Magnetic property measurements of GO's and MGOs were performed using a magnetometer. The SEM images of GO film, modified GO film, graphene porous film, and modified graphene porous film are shown in Fig. 5 [42]. The microstructure evolution of the unmodified GO films before (Fig. 5a) and after (Fig. 5c, e) the hydrazine-induced foaming process. Clearly, the GO film with highly-oriented GO sheets is converted to porous graphene film with random porous structures due to the excessive expansion derived from the weak interlayer interactions (Fig. 5c, e). The CS modified graphene (m-G) porous film (Fig. 5d, f) has distinct and continuous porous structures inherited from its precursor (Fig. 5b), which contrasts sharply the random structures of its unmodified counterpart (Fig. 5c, e). Additionally, some small pores are observed in the porous graphene film (Fig. 5f), which are beneficial for further decreasing the density of the porous film while retaining its reasonable strength.

XRD studies are mainly used to identify the formation, structure, and crystalline nature of MGOs. The XRD 2θ strong peak in the range 8°–12° indicates the formation of GO. By the magnetization, the crystalline property of GO is decreased by the increase of the mesoporous carbonaceous nature with alteration of the original position of the GO peak [47]. The XRD diffraction peaks are also used to identify the ferrite in MGOs. By decreasing the size of MGOs with increasing porosity, the positions of diffraction peaks shift to lower 2θ range [70].

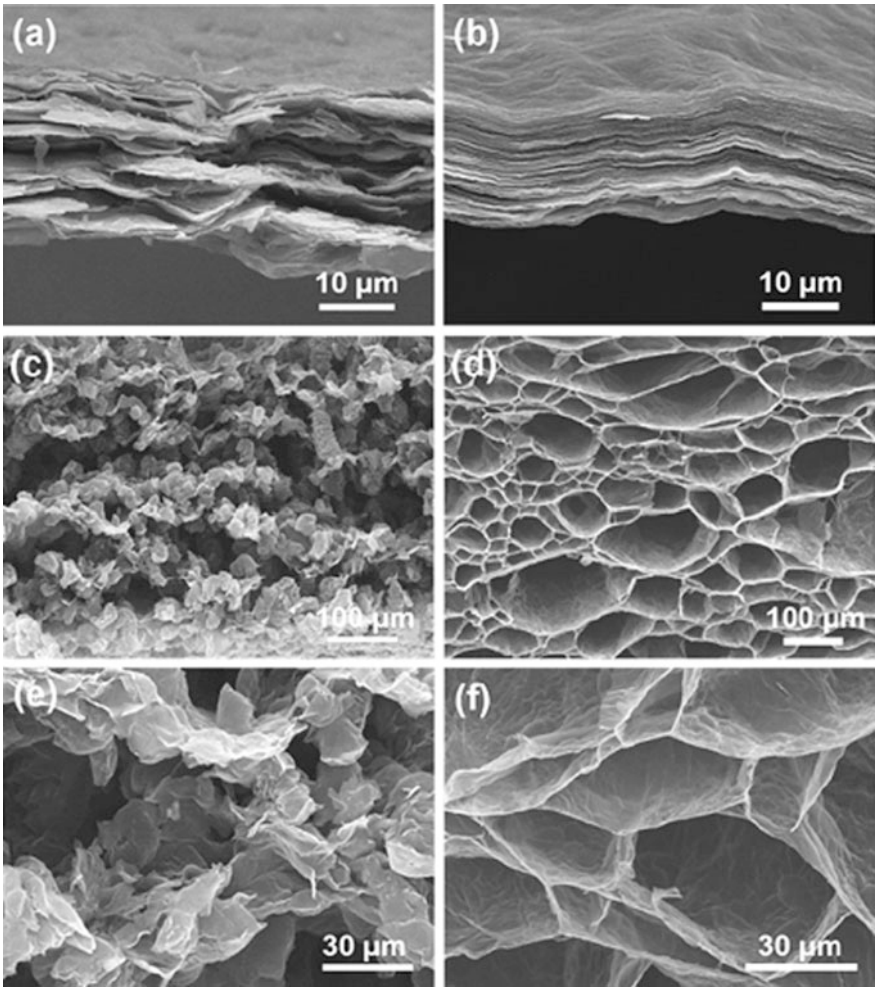

Fig. 5 SEM images of **a** GO film, **b** modified GO film, **c**, **e** graphene porous film, and **d**, **f** modified graphene porous film (reproduced from [42] with permission from Elsevier)

RS is an important technique to qualitatively identify the MGOs. As is known, the graphitic materials show two prominent Raman peaks around 1350 and 1600 cm^{-1} called the D and G bands. Here, the G band corresponds to the stretching vibrations of carbons at sp^2 hybridization, whereas the D band represents the vibrations of carbons at sp^3 hybridization, which can break the symmetry and selection rule [36]. By the magnetization of GO, these D and G bonds alter their positions, based on their principal interactions. But, in the case of nickel ferrite-rGO (rGONF), both the sp^2 domain (D) and sp^3 domain (G) carbons are shifted to lower range at $\sim$1303–1591 cm^{-1}, which indicates that both D and G band carbons are involved in the formation of reduced GO-based magnetic nanocomposite. The XPS is used to

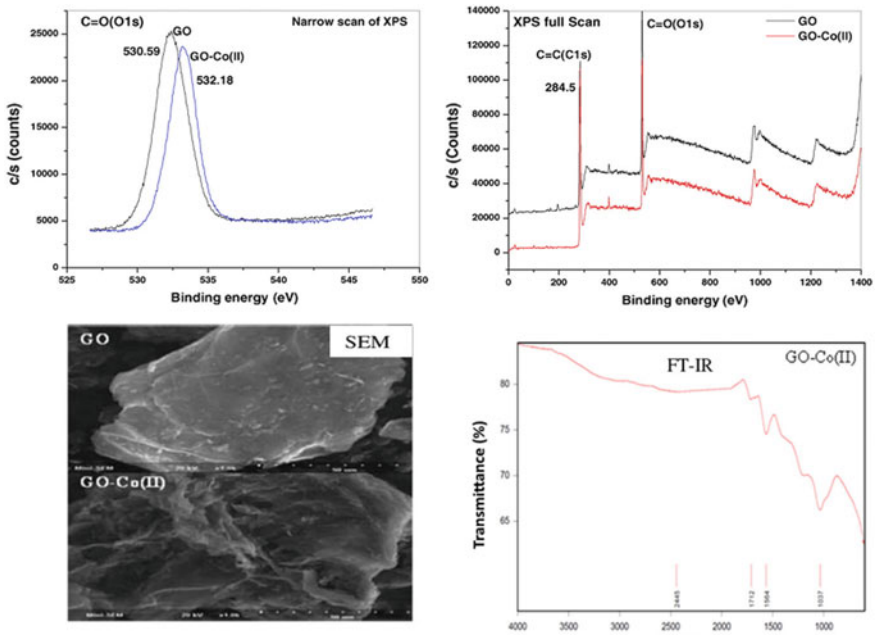

Fig. 6 XPS, SEM, FT-IR results of the Co(II)-loaded GO (reproduced from [40] with permission)

qualitative and quantitative identify the chemical composition of MGOs. The bonding energy peaks of 700–730 eV indicate the Fe peaks of magnetic materials.

The microscopic techniques, including SEM, TEM, and AFM, are used to measure the size of nanocomposites, MGOs, and their surface morphology, which is an important factor to know for the adsorption process. Their porous structure and surface area can be further evaluated by using (N_2) adsorption-desorption isotherms through BET analysis. The magnetic nature of MGOs is identified using the magnetic measurement system (MPMS). When the size of MGOs decreases to the nanoscale, it shows superparamagnetic nature. Lingamdinne et al. [36] confirmed the superparamagnetic property of magnetic nanocomposite by MT curves obtained at 1000 Oe magnetic field. They also observed the increase of superparamagnetic property by the reduction of nanocomposite [16]. The XPS, SEM, FT-IR of the Co(II)-GO were shown in Fig. 6.

5 Applications to Sustainable Water Purification

Graphene oxide is easily dispersed in water due to the plentiful hydrophilic (carboxylic, epoxide, and hydroxyl groups) groups on its surface. List of various GO based nanomaterials utilized for removal of heavy metal ions removal is given in

Table 1. Due to the hydrophilic nature of GO, it adsorbs the pollutants to stable complexes, causing difficulties for the separation and recovery of GO [96]. To overcome these difficulties of separation, magnetic functionalization of GO is an alternative solution [104]. Due to the magnetic particle has unique properties, they have been widely applied to the removal of various pollutants. Some researchers have developed magnetic graphene oxide composites for efficient applications, including water treatment, energy storage, and drug delivery [11]. Here, we review some research reports, and briefly critique the use of MGO based nanocomposites for the adsorption of heavy metals and radionuclides.

5.1 Heavy Metals Removal

Exposure to heavy metals can present serious health risks to human beings. For the purification of water, adsorption is an effective, economic, and easy operation technique, compared to conventional methods [54]. But it is limited, due to the difficulties in the filtration and regeneration of adsorbents. The use of magnetic materials for water purification can overcome the above difficulties, including the filtration and regeneration of adsorbents; therefore, many researchers have developed and widely used magnetic materials for the treatment of pollutants [60]. However, the nano metal ferrites show poor stability [47]. To overcome these difficulties, hybrid materials have been synthesized through magnetic ferrites and GO by the hydrothermal method. Due to the presence of epoxy, carboxylic, and hydroxyl functions at GO, they can enhance the adsorption of heavy metals [33]. The specific adsorption mechanisms of graphene oxide-based nanomaterials for metal ions removal are given in Table 2.

Chandra et al. [8] thru a chemical reaction developed 10 nm average size superparamagnetic magnetite reduced graphene oxide (M-RGO) composites. The M-RGO showed higher adsorption capacity over 99.9% for removal of both ionic states of Arsenic. Zhang et al. employed ferric hydroxide-GO composite for the magnificent adsorption of arsenate from water [98]. Here, high arsenate adsorption removal was observed over a pH range of 4–9 and reduced the arsenate concentration of contaminated water from 20 to 0.5 ppm. Water-soluble "magnetic graphene oxide nanocomposite" has been produced via a "copper catalyzed azide-alkyne cycloaddition", and was utilized for the adsorption removal of Pb (II), Cd(II), and Cu(II), from aqueous solutions [100]. The results found that the nanocomposite has the higher surface area and extraordinary removal capacity for heavy metals.

RGO–MnO_2 composites showed excellent Hg(II) uptake capacity [77]. The composite shows enhanced adsorption removal capacity compared to its base material. Liu et al. [43] employed an MGO for the successful removal of Co(II). The adsorption Co(II) on MGO was the rate-limiting kinetics, with "inner-sphere surface complexation" at low pH values. Meanwhile, at higher pH values, the removal mechanism of Co(II) was associated with inner-sphere surface

Table 1 List of various graphene oxide based nanomaterials utilized for removal of heavy metal ions removal

Metal ion	Adsorbent	Max. adsorption capacity (mg/g)	Conditions	Model (adsorption isotherm; kinetics)	Remarks
Cd	GO	1792.60	303 K; pH 4.0	Langmuir and Freundlich; pseudo second-order	• The equilibrium contact time is 120 min • The graphene oxide is generated by using amorphous graphite
	PAMAMs/GO	253.81	298 K; pH 5.0	Langmuir; pseudo second-order	• The adsorption process achieves equilibrium within 60 min • The adsorbent dosage is 0.1 g
	Few-layered GO nanosheets	106.30	303 K; pH 6.0	Langmuir	• The dosage of adsorbent is 0.1 g/L • The adsorption capacity is strongly based on pH and humic acid
	GO/cellulose membranes	26.8	298 K; pH 4.5	Langmuir; pseudo second-order	• Good adsorption and no precipitation of metal hydroxides • It can be reused up to ten cycles
Pb	Few-layered GO	842.00	293 K; pH 6.0	Langmuir	• pH value strongly affects the adsorption capacity • The adsorption capacity is strongly independent of ionic strength
	Graphene nanosheet	476.19	298 K; pH 6.2	Langmuir	• The equilibrium contact time is 35 min • The dosage of adsorbent is 40 mg/L
	Ag/GO	312.57	298 K; pH 5.3	Langmuir; pseudo second-order	• 0.05 mg of adsorbents used showed the maximum adsorption performance • The equilibrium time for the lead adsorption is 50 min
Cu	Chitosan/SH/GO	425.00	293 K; pH 5.0	Freundlich; pseudo second-order	• The dosage of adsorbents is 0.2 mg/mL • The adsorption efficiency is strongly dependent on pH, temperature and adsorbent dosage
	TiO_2/GO	45.20	293 K; pH 6.0	Langmuir	• The adsorption capacity is strongly based on the pH value
	GO aerogels	19.65	298 K; pH 6.2	Langmuir; pseudo second-order	• The dosage of adsorbents is 0.6 g/L • It involves ion exchange mechanism

(continued)

Table 1 (continued)

Metal ion	Adsorbent	Max. adsorption capacity (mg/g)	Conditions	Model (adsorption isotherm; kinetics)	Remarks
Cr	Chitosan/GO	310.40	318 K; pH 3.0	Redlich–Peterson/double exponential	• The adsorbent dosage is 0.5 g/L • Both internal and external diffusion take place effectively in the adsorption process
	Fe_3O_4/GO	32.33	293 K; pH 4.5	Langmuir; pseudo second-order	• pH value and ionic strength are the crucial factors to affect the adsorption capacities • The adsorbent dosage is 0.2 g/L

Adapted from [34] with permission from Elsevier

Table 2 Specific adsorption mechanisms of graphene oxide-based nanomaterials for metal ions removal

Graphene oxide-based nanomaterials	Adsorption mechanisms included for metal ions removal	Advantages	Drawbacks
Graphene oxide (GO)	• Electrostatic interactions • Ion exchange	• Good dispersion in water • Great colloidal constancy • Contains rich oxygenated functional groups	• A restricted number of sorption sites
Reduced graphene oxide (rGO)	• Electrostatic interactions • Lewis-base–acid mechanism	• Restoration of sp^2 domains • Better electron-transport properties	• Less oxygen-containing functional groups • Weaker colloidal stability
Magnetic graphene oxide nanocomposites	• Electrostatic interactions with graphene oxide • Interactions with the particles surface • Magnetic properties of the nanoparticles	• Bigger surface area compared to the pure GO • Increased number of binding sites compared to pure GO • Ease the recovery process from solutions	• Co-reduction of GO during the combination of the particles weakens the colloidal stability
Graphene oxide materials functionalized with organic molecules	• Electrostatic interactions • Complexation with organic molecules	• Bigger surface area compared to pure GO • Great colloidal stability • The greater number of functional groups ($–NH_2$, –OH)	• Large variations of the stability of the loaded molecules depending on the alteration approach physically or chemically

Reproduced from [34] with permission from Elsevier

complexation and precipitation. Co(II)-loaded MGO can be rapidly separated and recovered from aqueous solution by external magnetic field [43]. Liu et al. [44] reported a facile self-assembly of magnetic particles with GO through electrostatic interaction in the presence of 3-aminopropyltrimethoxysilane. The prepared porous MGO not only conventionally separated by a magnetic field but also enhanced the adsorption capacity of GO for Cr(VI) removal. They also concluded that the prepared MGO shows higher adsorption capacity than that of GO and Fe_3O_4. Bhunia et al. [6] developed a heterogeneous matrix of iron/iron oxide dispersed on RGO (RGO-FeO)/Fe_3O_4) that can be used for the effective adsorption of heavy metal ions, including Cr(VI), Hg(II), Pb(II), Cd(II), and As(III). Recently, Lingamdinne et al. employed porous inverse spinel composite (MGO) and porous inverse RMGO nanocomposites using nickel ferrite and GO, and applied them for the removal of Arsenic [38], Pb(II) and Cr(III) [35 36 37 39 40 41]. They also reported the as-prepared nanocomposites to show considerably enhanced adsorption capacity for Pb(II), Cr(III), As(III), and As(V), compared to that of GO. They stated that the adsorption efficiency of rMGO for As(III) and As(V) is 106.40 and 65.78 mg/g respectively was greater than that of MGO [38]. The adsorption process was thermodynamically favourable for the adsorption of Pb(II) and Cr(III) onto the nanocomposites and was spontaneous endothermic. But the As(III) and As(V) removal was enhanced with increased temperature up to 300 K, while it started decreasing with further increase of the temperature above 300 K. The unavailability of metal ions undergoing degradation process via bioprocesses and reactions chemically has led to the wider exposure to adsorption process and hence it is now considered as the most promising method to remove heavy metal ions [53].

Copper (II) ions can be removed effectively via the interaction between copper (II) ions and oxygen groups on GO which are positively charged and negatively charged respectively [92]. Besides, Pb(II), U(VI) and Co(II) ions can be adsorbed via the usage of GO as well [46]. For instance, powder X-ray diffraction (XRD), scanning electron microscopy (SEM), infrared spectroscopy (FT-IR) and X-ray photoelectron spectroscopy (XPS) are utilized to determine the adsorption characterization of GO towards copper, lead, zinc and cadmium. As a result, the largest adsorption capacities at pH 5 have been recorded as 294, 345, 530, 1119 mg/g for Cu(II), Zn(II), Cd(II) and Pb(II) respectively [76]. In addition, the adsorption capacities mentioned previously can be done in a wide range of pH values which are 3–7 for both Cu(II) and Pb(II), 4–8 for Cd(II) and 5–8 for Zn(II) [76]. It is studied that the removal of heavy metal ions via GO can be explained as the adsorption process is restricted chemically due to the participation of superficial complexity of metal ions with the presence of oxygen in the functional groups which lies on the surface of GO. As an example, cellulose hydrogel/GO possesses adsorption capacity of approximately 94 mg/g [9].

Furthermore, with the presence of metal oxides on GO and GNs, they are considered as high-performance adsorbents in the past [21]. For instance, the fabrication of GO–TiO_2 is implemented to remove Pb(II), Zn (II) and Cd(II) ions. Hence, the adsorption capacities of the GO–TiO_2 on the Pb(II), Zn (II) and Cd(II) ions at pH value of 5 are recorded at 65.8, 88.9 and 72.8 mg/g respectively [32].

The covalent bond which is securing the rGO and TiO_2 in the GO–TiO_2 has resulted in the poor electron-hole recombination and hence great amount of Cr(VI) can be reduced. Although different types of magnetic graphene composites have been utilized, to eradicate the separation difficulties, a combination of GO or GNs with magnetic materials is a good choice. The significant of the combination is to minimize the agglomeration and restacking of graphene sheets and at the same time increasing the surface area and adsorption efficiency [79].

Moreover, removal of cadmium ions and copper ions from wastewater can be done via fabrication of GNs through the method of modified Hummers [103]. For instance, at the condition of pH 6.0 ± 0.1 and temperature around 303 K, it is recorded that highest adsorption capacities of Co(II) and Cd(II) can be achieved with the value of 68.2 and 106.3 mg/g respectively. This has proven that the adsorption of heavy metal ions through GNs is depending on the ionic strength and pH. However, adsorption of chromium (VI) ions and chromium (III) ions can be done at the low range of pH levels but the adsorptions of copper (II) ions, lead (II) ions, and gold (III) ions are most likely to be occurring at higher range of pH levels [15].

Other than that, MMSP-GO to adsorb heavy metal ions such as Cd (II) and Pb(II) is worth studied as well. Once the synthesis of magnetic mesoporous silica comes with the functionalization with polyethyleneimine molecules, the conjugation of a great number of amine groups with carboxyl groups on the GO sheets could increase the affinity between the pollutants and mesoporous silica. Significant and effective data has been recorded for the MMSP-GO composites regarding its maximum adsorption capacities for Pb(II) and Cd(II) which are 333 and 167 mg/g respectively [90].

5.2 Organic Pollutants Removal

Presently, many process industries, including the paper, textile, paint, plastic, and leather industries, use pigments and dyes to colour their products, and excess of these colours end up in the discharge, which ultimately ends up as industrial effluent. These dyes are organic compounds, and the presence of dyes in an aquatic environment not only affects the aesthetics, it also inhibits the penetration of sunlight, and thus reduces photosynthesis for waterborne plants. Overall, the presence of dyes poses the threat of toxic materials, which are resistant to a chemical reaction in wastewaters, and which leads to cancer, mutagenesis, and other severe problems in human and aquatic creatures. The complicated chemical structures of dyes make these materials highly resistant to biodegradation [49]. Therefore, these dyes have to be removed efficiently before the effluent is discharged to the nearby aquatic environment.

In the last couple of years, magnetic nanoparticles have been extensively applied for the removal of toxic metal ions and organic pollutants. This is due to the features, like low toxicity, high chemical stability, and good magnetic properties.

Adsorbents based on magnetic nanoparticles are used in the removal of toxic dyes and heavy metals from aqueous solutions with precision and high accuracy [88]. However, the bare magnetic nanoparticles can easily be oxidized in atmospheric conditions. Therefore, to remedy these effects and increase the life of nanoparticles, researchers explored ways to coat or functionalize the magnetic nanoparticles and enhance the functional groups. In recent years, usage of GO-based magnetic nanoparticles as an adsorbent has increased. Association of graphene has resulted in high removal capacity of pollutants. Chandra et al. [8] reported that compared to free nanoparticles, RGO and GO embedded materials have shown higher binding capacity. Deng et al. [13] synthesized MGO and used it to investigate the simultaneous removal of Cd(II) and ionic dyes like orange gelb (OG) and methylene blue (MB). The maximum adsorption capacities reported for the removal of MB using graphene nanosheet/magnetite, magnetic rectorite/iron oxide, and multi-walled carbon nanotubes/Fe_2O_3, were 43.82, 31.18, and 42.30 mg/g, respectively. They also reported that the maximum sorption capacities of MGO (64.23 mg/g for MB, and 20.85 mg/g for OG) were much higher than those of "exfoliated graphene oxide" (17.3 mg/g for MB, and 5.98 for OG) used as adsorbent [58]. The maximum adsorption capacities reported for removal of dyes using bare iron oxide nanoparticles were 2.78 and 15.62 mg/g for MB and OG, respectively. Khurana et al. [28] investigated the "Eriochrome Black T" (EBT) adsorption from textile wastewater using MGO in a batch process. In this study, for the removal of toxic textile azo dye EBT, they synthesized MGO that was impregnated with α-Fe_2O_3. The maximum adsorption capacity for dye removal was reported to be 210.53 mg/g.

6 Conclusion and Future Perspective

This chapter indicates that adsorption using MGOs is becoming an alternative option to replace the conventional adsorbents used for water purification. It also shows that these MGO composites have comparable or even greater adsorption and regeneration capacity, compared to the available adsorbents and activated carbons. Moreover, the adsorbents coming out at long last with high adsorption efficiency for the handling of wastewater containing metal pollutants (heavy metals and radionuclides) and organic pollutants could be successfully implemented as beneficial to society.

The synthesis of graphene has been widely done by the latest and greatest method which is improved Hummers method. However, the experimental procedures to complete the fabrication of the graphene is time-consuming although the experimental complexity is considerably low. Therefore, replacement or removal of certain chemicals is required to be further discovered and studied to shorten the fabrication period and result in a better fabrication method.

The synthesis of graphene has been generally done by the enhanced Hummers technique. Applications are hindered due to the time-consuming methods for

fabricating the Graphene. Accordingly, appropriate techniques need to be discovered to reduce the fabrication period and thus enhance the performance of graphene obtained by these fabrications method. Another major hurdle in these applications is the scalability of these methods. Most of the recently reported studies are limited to lab scale experiments. Therefore, studies should also focus on the scalability of these applications from lab scale experiments into commercial industrial scale applications. It should also be noted that, industries which produce effluents and wastewater at a larger scale will consume higher quantities of GO's and MGO's, thus increasing the cost of operation to many folds. Therefore, the commercialized MGOS should be prepared in such a way that they can be re-used or regenerate with low operating cost.

Acknowledgments This work has been supported by the National Research Foundation (NRF) of Korea funded by the Ministry of Science, ICT & Future Planning (MSIP) (2017R1C1B5016656) of the Korea Government, Seoul, Korea.

References

1. Alvand M, Shemirani F (2016) Fabrication of Fe_3O_4@graphene oxide core-shell nanospheres for ferrofluid-based dispersive solid phase extraction as exemplified for Cd (II) as a model analyte. Microchim Acta 183:1749–1757. https://doi.org/10.1007/s00604-016-1805-8
2. Azimi A, Azari A, Rezakazemi M, Ansarpour M (2017) Removal of heavy metals from industrial wastewaters: a review. ChemBioEng Rev 4:37–59. https://doi.org/10.1002/cben.201600010
3. Balandin AA (2011) Thermal properties of graphene and nanostructured carbon materials. Nat Mater 10:569. https://doi.org/10.1038/nmat3064
4. Balandin AA, Ghosh S, Bao W, Calizo I, Teweldebrhan D, Miao F, Lau CN (2008) Superior thermal conductivity of single-layer graphene. Nano Lett 8:902–907
5. Berger C et al (2004) Ultrathin epitaxial graphite: 2D electron gas properties and a route toward graphene-based nanoelectronics. J Phys Chem B 108:19912–19916. https://doi.org/10.1021/jp040650f
6. Bhunia P, Kim G, Baik C, Lee H (2012) A strategically designed porous iron–iron oxide matrix on graphene for heavy metal adsorption. Chem Commun 48:9888
7. Bolotin KI et al (2008) Ultrahigh electron mobility in suspended graphene. Solid State Commun 146:351–355. https://doi.org/10.1016/j.ssc.2008.02.024
8. Chandra V, Park J, Chun Y, Lee JW, Hwang I-C, Kim KS (2010) Water-dispersible magnetite-reduced graphene oxide composites for arsenic removal. ACS Nano 4:3979–3986. https://doi.org/10.1021/nn1008897
9. Chen X, Zhou S, Zhang L, You T, Xu F (2016) Adsorption of heavy metals by graphene oxide/cellulose hydrogel prepared from NaOH/urea aqueous solution. Mater 9:582
10. Cheng Z, Liao J, He B, Zhang F, Zhang F, Huang X, Zhou L (2015) One-step fabrication of graphene oxide enhanced magnetic composite gel for highly efficient dye adsorption and catalysis. ACS Sustain Chem Eng 3:1677–1685
11. Chung C, Kim Y-K, Shin D, Ryoo S-R, Hong BH, Min D-H (2013) Biomedical applications of graphene and graphene oxide. Acc Chem Res 46:2211–2224
12. Dasari BL, Nouri JM, Brabazon D, Naher S (2017) Graphene and derivatives—synthesis techniques, properties and their energy applications. Energy 140:766–778. https://doi.org/10.1016/j.energy.2017.08.048

13. Deng J-H, Zhang X-R, Zeng G-M, Gong J-L, Niu Q-Y, Liang J (2013) Simultaneous removal of Cd (II) and ionic dyes from aqueous solution using magnetic graphene oxide nanocomposite as an adsorbent. Chem Eng J 226:189–200
14. Deng J-H, Zhang X-R, Zeng G-M, Gong J-L, Niu Q-Y, Liang J (2013) Simultaneous removal of Cd(II) and ionic dyes from aqueous solution using magnetic graphene oxide nanocomposite as an adsorbent. Chem Eng J 226:189–200
15. Duru I, Ege D, Kamali AR (2016) Graphene oxides for removal of heavy and precious metals from wastewater. J Mater Sci 51:6097–6116
16. Fan Z, Wang K, Wei T, Yan J, Song L, Shao B (2010) An environmentally friendly and efficient route for the reduction of graphene oxide by aluminum powder. Carbon 48:1686–1689
17. Gollavelli G, Chang C-C, Ling Y-C (2013) Facile synthesis of smart magnetic graphene for safe drinking water: heavy metal removal and disinfection control. ACS Sustain Chem Eng 1:462–472
18. Gomez-Navarro C, Burghard M, Kern K (2008) Elastic properties of chemically derived single graphene sheets. Nano Lett 8:2045–2049. https://doi.org/10.1021/nl801384y
19. Hashim N et al (2016) A brief review on recent graphene oxide-based material nanocomposites: synthesis and applications. J Mater Environ Sci 7:3225–3243
20. Hu X-J et al (2013) Removal of Cu(II) ions from aqueous solution using sulfonated magnetic graphene oxide composite. Sep Purif Technol 108:189–195
21. Hur J, Shin J, Yoo J, Seo YS (2015) Competitive adsorption of metals onto magnetic graphene oxide: comparison with other carbonaceous adsorbents. The Sci World J 2015:1–11. https://doi.org/10.1155/2015/836287
22. Abbas A, Al-Amer AM, Laoui T, Al-Marri MJ, Nasser MS, Khraisheh M, Atieh MA (2016) Heavy metal removal from aqueous solution by advanced carbon nanotubes: critical review of adsorption applications. Sep Purif Technol 157:141–161
23. Ionita M, Vlăsceanu GM, Watzlawek AA, Voicu SI, Burns JS, Iovu H (2017) Graphene and functionalized graphene: extraordinary prospects for nanobiocomposite materials. Compos B Eng 121:34–57
24. Jiang J-W, Lan J, Wang J-S, Li B (2010) Isotopic effects on the thermal conductivity of graphene nanoribbons: localization mechanism. J Appl Phys 107:054314. https://doi.org/10.1063/1.3329541
25. Karri RR, Sahu JN (2018) Modeling and optimization by particle swarm embedded neural network for adsorption of zinc (II) by palm kernel shell based activated carbon from aqueous environment. J Environ Manage 206:178–191
26. Karri RR, Jayakumar N, Sahu J (2017) Modelling of fluidised-bed reactor by differential evolution optimization for phenol removal using coconut shells based activated carbon. J Mol Liq 231:249–262
27. Karri RR, Sahu JN, Jayakumar NS (2017) Optimal isotherm parameters for phenol adsorption from aqueous solutions onto coconut shell based activated carbon: error analysis of linear and non-linear methods. J Taiwan Inst Chem Eng 80:472–487
28. Khurana I, Shaw AK, Bharti, Khurana JM, Rai PK (2018) Batch and dynamic adsorption of Eriochrome Black T from water on magnetic graphene oxide: experimental and theoretical studies. J Environ Chem Eng 6:468–477
29. Kou L, Tang C, Guo W, Chen C (2011) Tunable magnetism in strained graphene with topological line defect. ACS Nano 5:1012–1017. https://doi.org/10.1021/nn1024175
30. Krane N (2011) Selected topics in physics: physics of nanoscale carbon. Freie Universität, Berlin
31. Lee C, Wei X, Li Q, Carpick R, Kysar Jeffrey W, Hone J (2009) Elastic and frictional properties of graphene. Physica Status Solidi (b) 246:2562–2567. https://doi.org/10.1002/pssb.200982329
32. Lee Y-C, Yang J-W (2012) Self-assembled flower-like TiO_2 on exfoliated graphite oxide for heavy metal removal. J Ind Eng Chem 18:1178–1185

33. Li J, Guo S, Zhai Y, Wang E (2009) Nafion–graphene nanocomposite film as enhanced sensing platform for ultrasensitive determination of cadmium. Electrochem Commun 11:1085–1088
34. Lim JY, Mubarak NM, Abdullah EC, Nizamuddin S, Khalid M, Inamuddin (2018) Recent trends in the synthesis of graphene and graphene oxide based nanomaterials for removal of heavy metals—a review. J Ind Eng Chem. https://doi.org/10.1016/j.jiec.2018.05.028
35. Lingamdinne L, Kim I-S, Ha J-H, Chang Y-Y, Koduru J, Yang J-K (2017) Enhanced adsorption removal of Pb(II) and Cr(III) by using nickel ferrite-reduced graphene oxide nanocomposite. Metals 7:225
36. Lingamdinne LP, Choi Y-L, Kim I-S, Yang J-K, Koduru JR, Chang Y-Y (2017) Preparation and characterization of porous reduced graphene oxide based inverse spinel nickel ferrite nanocomposite for adsorption removal of radionuclides. J Hazard Mater 326:145–156
37. Lingamdinne LP, Koduru JR, Chang Y-Y, Karri RR (2018) Process optimization and adsorption modeling of Pb(II) on nickel ferrite-reduced graphene oxide nano-composite. J Mol Liq 250:202–211
38. Lingamdinne LP, Choi Y-L, Kim I-S, Chang Y-Y, Koduru JR, Yang J-K (2016) Porous graphene oxide based inverse spinel nickel ferrite nanocomposites for the enhanced adsorption removal of arsenic. RSC Adv 6(77):73776–73789
39. Lingamdinne LP, Koduru JR, Choi Y-L, Chang Y-Y, Yang J-K (2016) Studies on removal of Pb(II) and Cr(III) using graphene oxide based inverse spinel nickel ferrite nano-composite as sorbent. Hydrometallurgy 165:64–72
40. Lingamdinne LP, Koduru JR, Roh H, Choi Y-L, Chang Y-Y, Yang J-K (2016) Adsorption removal of Co(II) from waste-water using graphene oxide. Hydrometallurgy 165:90–96
41. Lingamdinne LP, Roh H, Choi Y-L, Koduru JR, Yang J-K, Chang Y-Y (2015) Influencing factors on sorption of TNT and RDX using rice husk biochar. J Ind Eng Chem 32:178–186
42. Liu J, Zhang H-B, Liu Y, Wang Q, Liu Z, Mai Y-W, Yu Z-Z (2017) Magnetic, electrically conductive and lightweight graphene/iron pentacarbonyl porous films enhanced with chitosan for highly efficient broadband electromagnetic interference shielding. Compos Sci Technol 151:71–78. https://doi.org/10.1016/j.compscitech.2017.08.005
43. Liu M, Chen C, Hu J, Wu X, Wang X (2011) Synthesis of magnetite/graphene oxide composite and application for cobalt(ii) removal. J Phys Chem C 115:25234–25240
44. Liu M, Wen T, Wu X, Chen C, Hu J, Li J, Wang X (2013) Synthesis of porous Fe_3O_4 hollow microspheres/graphene oxide composite for Cr(vi) removal. Dalton Trans 42:14710
45. Liu P, Yao Z, Zhou J (2015) Preparation of reduced graphene oxide/$NiO{\cdot}4ZnO{\cdot}4CoO{\cdot}2Fe_2O_4$ nanocomposites and their excellent microwave absorption properties. Ceram Int 41:13409–13416
46. Liu, ZJ, Yang, JW, Li, CZ, Li, JX, Jiang, YJ, Dong, YH, Li, YY (2014) Adsorption of Co (II), Ni (II), Pb (II) and U (VI) from aqueous solutions using polyaniline/graphene oxide composites. Korean Chem Eng Res 52(6):781–788. https://doi.org/10.9713/kcer.2014.52.6.781
47. Maaz K, Karim S, Mumtaz A, Hasanain SK, Liu J, Duan JL (2009) Synthesis and magnetic characterization of nickel ferrite nanoparticles prepared by co-precipitation route. J Magn Magn Mater 321:1838–1842
48. Mesbah M, Shahsavari S, Soroush E, Rahaei N, Rezakazemi M (2018) Accurate prediction of miscibility of CO_2 and supercritical CO_2 in ionic liquids using machine learning. J CO_2 Utilization 25:99–107. https://doi.org/10.1016/j.jcou.2018.03.004
49. Mokhtari P, Ghaedi M, Dashtian K, Rahimi M, Purkait M (2016) Removal of methyl orange by copper sulfide nanoparticles loaded activated carbon: kinetic and isotherm investigation. J Mol Liq 219:299–305
50. Muzyka R, Kwoka M, Smędowski Ł, Díez N, Gryglewicz G (2017) Oxidation of graphite by different modified Hummers methods. New Carbon Mater 32:15–20. https://doi.org/10.1016/S1872-5805%5b17%5d60102-1
51. Novoselov KS et al (2004) Electric field effect in atomically thin carbon films. Science 306:666–669

52. Novoselov KS, Jiang D, Schedin F, Booth TJ, Khotkevich VV, Morozov SV, Geim AK (2005) Two-dimensional atomic crystals. Proc Natl Acad Sci U S A 102:10451
53. Nupearachchi CN, Mahatantila K, Vithanage M (2017) Application of graphene for decontamination of water implications for sorptive removal. Groundwater Sustain Dev 5:206–215. https://doi.org/10.1016/j.gsd.2017.06.006
54. Oraby EA, Eksteen JJ (2015) The leaching of gold, silver and their alloys in alkaline glycine–peroxide solutions and their adsorption on carbon. Hydrometallurgy 152:199–203
55. Peng Y, Ji J, Chen D (2015) Ultrasound assisted synthesis of ZnO/reduced graphene oxide composites with enhanced photocatalytic activity and anti-photocorrosion. Appl Surf Sci 356:762–768
56. Pettes MT, Jo I, Yao Z, Shi L (2011) Influence of polymeric residue on the thermal conductivity of suspended bilayer graphene. Nano Lett 11:1195–1200. https://doi.org/10.1021/nl104156y
57. Phiri J, Gane P, Maloney TC (2017) General overview of graphene: production, properties and application in polymer composites. Mater Sci Eng B 215:9–28. https://doi.org/10.1016/j.mseb.2016.10.004
58. Ramesha G, Kumara AV, Muralidhara H, Sampath S (2011) Graphene and graphene oxide as effective adsorbents toward anionic and cationic dyes. J Colloid Interface Sci 361:270–277
59. Razavi SMR, Rezakazemi M, Albadarin AB, Shirazian S (2016) Simulation of CO_2 absorption by solution of ammonium ionic liquid in hollow-fiber contactors. Chem Eng Process Process Intensification 108:27–34. https://doi.org/10.1016/j.cep.2016.07.001
60. Reddy DHK, Lee S-M (2013) Application of magnetic chitosan composites for the removal of toxic metal and dyes from aqueous solutions. Adv Coll Interface Sci 201–202:68–93
61. Rezakazemi M, Dashti A, Riasat Harami H, Hajilari N, Inamuddin (2018) Fouling-resistant membranes for water reuse. Environ Chem Lett 1–49. https://doi.org/10.1007/s10311-018-0717-8
62. Rezakazemi M, Ghafarinazari A, Shirazian S, Khoshsima A (2013) Numerical modeling and optimization of wastewater treatment using porous polymeric membranes. Polym Eng Sci 53:1272–1278. https://doi.org/10.1002/pen.23375
63. Rezakazemi M, Khajeh A, Mesbah M (2018) Membrane filtration of wastewater from gas and oil production. Environ Chem Lett 16:367–388. https://doi.org/10.1007/s10311-017-0693-4
64. Rezakazemi M, Shirazian S, Ashrafizadeh SN (2012) Simulation of ammonia removal from industrial wastewater streams by means of a hollow-fiber membrane contactor. Desalination 285:383–392. https://doi.org/10.1016/j.desal.2011.10.030
65. Rezakazemi M, Zhang Z (2018) 2.29 Desulfurization materials A2. In: Ibrahim D (ed) Comprehensive energy systems. Elsevier, Oxford, pp 944–979. https://doi.org/10.1016/B978-0-12-809597-3.00263-7
66. Sanes J, Avilés M-D, Saurín N, Espinosa T, Carrión F-J, Bermúdez M-D (2017) Synergy between graphene and ionic liquid lubricant additives. Tribol Int 116:371–382. https://doi.org/10.1016/j.triboint.2017.07.030
67. Sarı A, Tuzen M, Soylak M (2007) Adsorption of Pb(II) and Cr(III) from aqueous solution on Celtek clay. J Hazard Mater 144:41–46
68. Sarkar SK, Raul KK, Pradhan SS, Basu S, Nayak A (2014) Magnetic properties of graphite oxide and reduced graphene oxide. Physica E 64:78–82. https://doi.org/10.1016/j.physe.2014.07.014
69. Saurín N, Sanes J, Bermúdez M-D (2016) New graphene/ionic liquid nanolubricants. Mater Today Proc 3:S227–S232. https://doi.org/10.1016/j.matpr.2016.02.038
70. Senthilkumar B, Kalai Selvan R, Vinothbabu P, Perelshtein I, Gedanken A (2011) Structural, magnetic, electrical and electrochemical properties of $NiFe_2O_4$ synthesized by the molten salt technique. Mater Chem Phys 130:285–292
71. Seol JH et al (2010) Two-dimensional phonon transport in supported graphene. Science 328:213

72. Sepioni M et al (2010) Limits on intrinsic magnetism in graphene. Phys Rev Lett 105:207205
73. Sharma R, Baik JH, Perera CJ, Strano MS (2010) Anomalously large reactivity of single graphene layers and edges toward electron transfer chemistries. Nano Lett 10:398–405. https://doi.org/10.1021/nl902741x
74. She X, Zhang X, Liu J, Li L, Yu X, Huang Z, Shang S (2015) Microwave-assisted synthesis of Mn_3O_4 nanoparticles@reduced graphene oxide nanocomposites for high performance supercapacitors. Mater Res Bull 70:945–950
75. Shirazian S, Rezakazemi M, Marjani A, Moradi S (2012) Hydrodynamics and mass transfer simulation of wastewater treatment in membrane reactors. Desalination 286:290–295. https://doi.org/10.1016/j.desal.2011.11.039
76. Sitko R et al (2013) Adsorption of divalent metal ions from aqueous solutions using graphene oxide. Dalton Trans 42:5682–5689. https://doi.org/10.1039/C3DT33097D
77. Sreeprasad TS, Maliyekkal SM, Lisha KP, Pradeep T (2011) Reduced graphene oxide–metal/metal oxide composites: facile synthesis and application in water purification. J Hazard Mater 186:921–931
78. Stankovich S et al (2006) Graphene-based composite materials. Nature 442:282–286
79. Sun H, Cao L, Lu L (2011) Magnetite/reduced graphene oxide nanocomposites: one step solvothermal synthesis and use as a novel platform for removal of dye pollutants. Nano Res 4:550–562
80. Sun L, Wang G, Hao R, Han D, Cao S (2015) Solvothermal fabrication and enhanced visible light photocatalytic activity of Cu_2O-reduced graphene oxide composite microspheres for photodegradation of Rhodamine B. Appl Surf Sci 358:91–99
81. Sur UK (2012) Graphene: a rising star on the horizon of materials science. Int J Electrochem 2012: Article ID 237689, 12 pages. http://dx.doi.org/10.1155/2012/237689
82. Szabo T, Nánai L, Nesztor D, Barna B, Malina O, Tombácz E (2018) A simple and scalable method for the preparation of magnetite/graphene oxide nanocomposites under mild conditions. Adv Mater Sci Eng 2018:1–11
83. Tangahu BV, Sheikh Abdullah SR, Basri H, Idris M, Anuar N, Mukhlisin M (2011) A review on heavy metals (As, Pb, and Hg) uptake by plants through phytoremediation. Int J Chem Eng 2011:1–31
84. Tsoukleri G et al (2009) Subjecting a graphene monolayer to tension and compression. Small 5:2397–2402. https://doi.org/10.1002/smll.200900802
85. Ugeda MM, Brihuega I, Guinea F, Gómez-Rodríguez JM (2010) Missing atom as a source of carbon magnetism. Phys Rev Lett 104:096804
86. Urbas K, Aleksandrzak M, Jedrzejczak M, Jedrzejczak M, Rakoczy R, Chen X, Mijowska E (2014) Chemical and magnetic functionalization of graphene oxide as a route to enhance its biocompatibility. Nanoscale Res Lett 9:656
87. Vozmediano MAH, López-Sancho MP, Stauber T, Guinea F (2005) Local defects and ferromagnetism in graphene layers. Phys Rev B 72:155121
88. Wang H et al (2012) Fe nanoparticle-functionalized multi-walled carbon nanotubes: one-pot synthesis and their applications in magnetic removal of heavy metal ions. J Mater Chem 22:9230
89. Wang Y, Huang Y, Song Y, Zhang X, Ma Y, Liang J, Chen Y (2009) Room-temperature ferromagnetism of graphene. Nano Lett 9:220–224. https://doi.org/10.1021/nl802810g
90. Wang Y, Liang S, Chen B, Guo F, Yu S, Tang Y (2013) Synergistic removal of Pb (II), Cd (II) and humic acid by Fe_3O_4@ mesoporous silica-graphene oxide composites. PLoS One 8: e65634
91. Xie L et al (2011) Room temperature ferromagnetism in partially hydrogenated epitaxial graphene. Appl Phys Lett 98:193113. https://doi.org/10.1063/1.3589970
92. Yang S-T et al (2010) Folding/aggregation of graphene oxide and its application in Cu^{2+} removal. J Colloid Interface Sci 351:122–127. https://doi.org/10.1016/j.jcis.2010.07.042
93. Yang Y, Asiri AM, Tang Z, Du D, Lin Y (2013) Graphene based materials for biomedical applications. Mater Today 16:365–373. https://doi.org/10.1016/j.mattod.2013.09.004

94. Yazyev OV (2008) Magnetism in disordered graphene and irradiated graphite. Phys Rev Lett 101:037203
95. Yazyev OV, Helm L (2007) Defect-induced magnetism in graphene. Phys Rev B 75:125408
96. Yu S, Wang X, Tan X, Wang X (2015) Sorption of radionuclides from aqueous systems onto graphene oxide-based materials: a review. Inorg Chem Front 2:593–612
97. Zhang C, Shao Y, Zhu L, Wang J, Wang J, Guo Y (2017) Acute toxicity, biochemical toxicity and genotoxicity caused by 1-butyl-3-methylimidazolium chloride and 1-butyl-3-methylimidazolium tetrafluoroborate in zebrafish (Danio rerio) livers. Environ Toxicol Pharmacol 51:131–137
98. Zhang K, Dwivedi V, Chi C, Wu J (2010) Graphene oxide/ferric hydroxide composites for efficient arsenate removal from drinking water. J Hazard Mater 182:162–168
99. Zhang P, Ma L, Fan F, Zeng Z, Peng C, Loya PE, Liu Z, Gong Y, Zhang J, Zhang X Ajayan PM (2014) Fracture toughness of graphene. Nat Commun 5:3782
100. Zhang W, Shi X, Zhang Y, Gu W, Li B, Xian Y (2013) Synthesis of water-soluble magnetic graphene nanocomposites for recyclable removal of heavy metal ions. J Mater Chem A 1:1745–1753
101. Zhang Y-Y, Pei Q-X, Cheng Y, Zhang Y-W, Zhang X (2017) Thermal conductivity of penta-graphene: the role of chemical functionalization. Comput Mater Sci 137:195–200. https://doi.org/10.1016/j.commatsci.2017.05.042
102. Zhang Y, Small JP, Pontius WV, Kim P (2005) Fabrication and electric-field-dependent transport measurements of mesoscopic graphite devices. Appl Phys Lett 86:073104. https://doi.org/10.1063/1.1862334
103. Zhao G, Li J, Ren X, Chen C, Wang X (2011) Few-layered graphene oxide nanosheets as superior sorbents for heavy metal ion pollution management. Environ Sci Technol 45:10454–10462
104. Zhu J, He J, Du X, Lu R, Huang L, Ge X (2011) A facile and flexible process of β-cyclodextrin grafted on Fe_3O_4 magnetic nanoparticles and host–guest inclusion studies. Appl Surf Sci 257:9056–9062
105. Zhu J et al (2012) Magnetic graphene nanoplatelet composites toward arsenic removal. ECS J Solid State Sci Technol 1:M1–M5
106. Zhu Y, Murali S, Cai W, Li X, Suk Ji W, Potts Jeffrey R, Ruoff Rodney S (2010) Graphene and graphene oxide: synthesis, properties, and applications. Adv Mater 22:3906–3924. https://doi.org/10.1002/adma.201001068